

# An Alkali Metal-Capped Cerium(IV) Imido Complex

Lukman A. Solola, Alexander V. Zabula, Walter L. Dorfner, Brian C. Manor, Patrick J. Carroll, and Eric J. Schelter\*

P. Roy and Diana T. Vagelos Laboratories, Department of Chemistry, University of Pennsylvania, 231 South 34th Street, Philadelphia, Pennsylvania 19104, United States

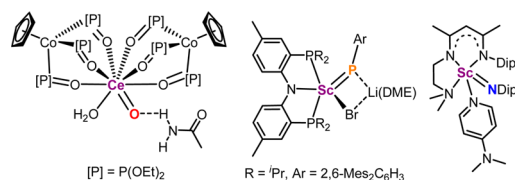
**S** Supporting Information

**ABSTRACT:** Structurally authenticated, terminal lanthanide–ligand multiple bonds are rare and expected to be highly reactive. Even capped with an alkali metal cation, poor orbital energy matching and overlap of metal and ligand valence orbitals should result in strong charge polarization within such bonds. We expand on a new strategy for isolating terminal lanthanide–ligand multiple bonds using cerium(IV) complexes. In the current case, our tailored tris(hydroxylamino) ligand framework,  $\text{TriNOx}^{3-}$ , provides steric protection against ligand scrambling and metal complex oligomerization and electronic protection against reduction. This strategy culminates in isolation of the first formal  $\text{Ce}=\text{N}$  bonded moiety in the complex  $[\text{K}(\text{DME})_2][\text{Ce}=\text{N}(3,5\text{-(CF}_3)_2\text{C}_6\text{H}_3)(\text{TriNOx})]$ , whose  $\text{Ce}=\text{N}$  bond is the shortest known at 2.119(3) Å.

d-Block transition metal complexes containing metal–ligand multiple bonds are essential in studies of small-molecule activation.<sup>1</sup> Interest in these complexes is driven by their synthetic applications, such as in group transfer of methylidene, imido, and phosphinidene moieties<sup>2</sup> and in multiple bond metathesis.<sup>3</sup> Likewise, a large number of synthetic procedures have been developed for the synthesis of complexes containing actinide–ligand multiple bonds.<sup>4</sup> However, the chemistry of complexes that contain metal–ligand multiple bonds with rare earth elements is comparatively underdeveloped.<sup>5</sup> Rare earth metal–ligand multiple bonds are understood to be reactive due to their low covalency and strong charge polarization that originates from the energy mismatch and poor spatial overlap between the valence rare earth metal and ligand orbitals.<sup>6</sup> These complexes can also oligomerize or access bimolecular decomposition pathways upon formation due to the large sizes and high Lewis acidities of the cations.<sup>7</sup>

It is of interest to prepare new complexes containing rare earth metal–ligand multiple bonds to expand on this important class of compounds and define the reactivities enabled by the unique characteristics of the ions. For example, a recently isolated  $\text{Ce}^{\text{IV}}=\text{O}$  complex, the first example of a  $\text{Ce}(\text{IV})$  metal–ligand multiple bond, was shown to possess strong nucleophilic and oxidizing properties (Scheme 1).<sup>5c</sup> Scandium complexes containing phosphinidene<sup>5b</sup> and imido<sup>8</sup> ligands have also been reported. A recent report of a chelating nucleophilic carbene complex of  $\text{Ce}(\text{IV})$ , wherein the carbene is electronically supported by heteroatoms, featured a short cerium–carbene bond.<sup>9</sup>

## Scheme 1. Isolated Complexes Containing Rare Earth Metal–Ligand Multiple Bonds



We recently reported the coordination chemistry of a tripodal, anionic hydroxylamino ligand framework,  $\text{TriNOx}^{3-}$ , with rare earth cations (Scheme 2).<sup>10</sup> We also demonstrated that a combination of both the electronic and steric characteristics of  $\text{TriNOx}^{3-}$  allows for the stabilization of tetravalent Ce with anionic ligands.<sup>10b</sup> For example, the  $\text{Ce}(\text{III/IV})$  redox wave for the complex was measured at  $-0.96$  V vs  $\text{Fc}/\text{Fc}^+$ , which compared favorably to the  $\text{Ce}(\text{III/IV})$  couple at  $+0.35$  V measured for  $\text{Ce}[\text{N}(\text{SiMe}_3)_2]_3$ .<sup>11</sup>

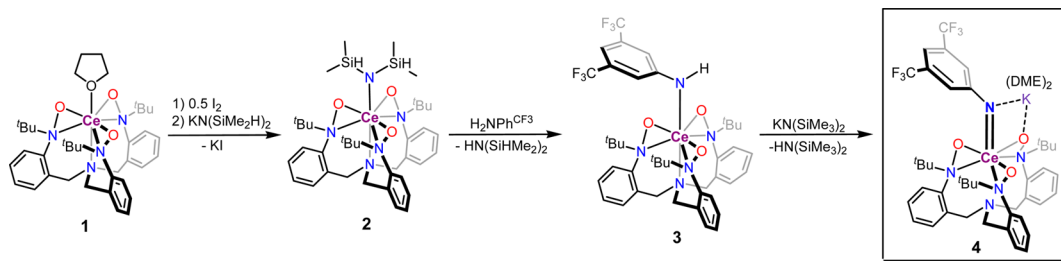
For the current work, we reasoned that the  $\text{TriNOx}^{3-}$  ligand framework could offer advantages toward the isolation of  $\text{Ce}^{4+}=\text{E}$  moieties ( $\text{E} = \text{N}, \text{O}, \text{P}$ ). Our hypothesis was that the established ability of the  $\text{TriNOx}^{3-}$  framework to stabilize  $\text{Ce}(\text{IV})$  and its steric properties would furnish a discrete terminal 1:1  $\text{Ce}(\text{IV})$ –imido complex. We also expected that Ce in the tetravalent oxidation state would provide a better electrostatic match for the dianionic imido ligand compared to  $\text{Ce}(\text{III})$ . Our synthetic strategy for the isolation of a  $\text{Ce}^{\text{IV}}=\text{N}$  complex was predicated on the deprotonation of an appropriate anilide complex. This route was previously employed for the generation of bridging  $\text{Ln}^{\text{III}}=\text{N}$  complexes ( $\text{Ln} = \text{Sm}, \text{Yb}$ ).<sup>5e,f</sup>

In pursuit of the anilide complex, we sought a suitable  $\text{Ce}^{\text{IV}}(\text{TriNOx})$  complex with a sufficiently basic ligand. The salt metathesis reaction between  $\text{Ce}(\text{TriNOx})\text{I}$ , generated *in situ* by oxidation of  $\text{Ce}(\text{THF})(\text{TriNOx})$  (**1**)<sup>10b</sup> with  $\text{I}_2$ , and  $\text{KN}(\text{SiHMe}_2)_2$  produced  $\text{Ce}[\text{N}(\text{SiHMe}_2)_2](\text{TriNOx})$  (**2**) in moderate (25%) crystalline yield (Scheme 2). <sup>1</sup>H NMR spectroscopy of **2** displayed a characteristic septet centered at  $\delta = 6.71$  ppm, which was slightly downfield shifted from the related signal observed for the homoleptic compound  $\text{Ce}[\text{N}(\text{SiHMe}_2)_2]_4$  ( $\delta = 6.01$  ppm).<sup>12</sup> The <sup>1</sup>H NMR data for **2** were similarly consistent with a  $\text{Ce}(\text{IV})$  complex. A pair of doublets centered at  $\delta = 4.46$  and 2.34 ppm were assigned to the diastereotopic benzylic protons of the  $\text{TriNOx}^{3-}$  ligand. The molecular structure of **2** was determined by an X-ray diffraction

Received: March 30, 2016

Published: May 10, 2016

## Scheme 2. Synthesis of Cerium(IV) Anilide and Imido Complexes 3 and 4



study (Figures 1a and S1). The Ce(1)–N(5) bond length of 2.353(5) Å was longer than the average Ce–N length of 2.247 Å reported for Ce[N(SiHMe<sub>2</sub>)<sub>2</sub>]<sub>4</sub>,<sup>12</sup> possibly due to the steric demand of the TriNOx<sup>3-</sup> framework. The Ce–O<sub>TriNOx</sub> bond lengths in 2 ranged between 2.167(4) and 2.191(4) Å and were consistent with those of reported Ce<sup>IV</sup>(TriNOx) complexes.<sup>10b</sup>

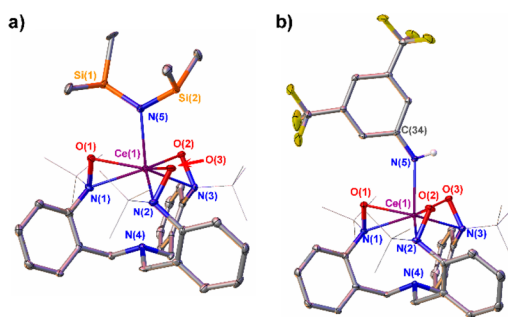


**Figure 1.** Thermal ellipsoid plots of (a) 2 (one of two independent molecules, see Supporting Information for details) and (b) 3·THF shown at the 30% probability level. Interstitial solvent molecules and hydrogen atoms, except for the anilide proton in 3·THF, have been omitted for clarity. *tert*-Butyl groups are depicted using a wire model. Selected bond distances (Å) and angles (deg) for 3·THF: Ce(1)–O(1) 2.184(2), Ce(1)–O(2) 2.158(3), Ce(1)–O(3) 2.203(2), Ce(1)–N(1) 2.510(3), Ce(1)–N(2) 2.512(3), Ce(1)–N(3) 2.541(3), Ce(1)–N(5) 2.379(3); Ce(1)–N(5)–C(34) 143.3(2).

Treating 2 with an *n*-pentane solution of 3,5-bis(trifluoromethyl)aniline afforded an analytically pure, insoluble black powder in 93% isolated yield that was identified as Ce[NH(3,5-(CF<sub>3</sub>)<sub>2</sub>C<sub>6</sub>H<sub>3</sub>)](TriNOx) (3) (Scheme 2). A diagnostic feature of complex 3 was its singlet at  $\delta = 6.57$  ppm in the <sup>1</sup>H NMR spectrum recorded in deuterated chloroform, assigned to the anilide proton. The IR spectrum of 3 showed an absorption band at  $\nu = 3311$  cm<sup>-1</sup>, which was assigned to the N–H oscillator. This value was consistent with that observed for the titanium(IV) anilide complex, (C<sub>5</sub>H<sub>5</sub>)<sub>2</sub>TiCl<sub>2</sub>(NHPh) ( $\nu = 3330$  cm<sup>-1</sup>).<sup>13</sup> Complex 3 represents the first crystallographically characterized Ce(IV)–anilide complex (Figure 1b). The internal bond lengths and angles for 3 were largely consistent with those found in complex 2, except for a shortening of the Ce–N<sub>TriNOx</sub> interactions (~0.05 Å) that was observed in 3 compared to 2. Also, the Ce–N<sub>anilide/amide</sub> bond length of 3 (2.379(3) Å) was only slightly longer than those measured in 2 (2.353(5) and 2.370(5) Å).

Addition of an equimolar amount of KN(SiMe<sub>3</sub>)<sub>2</sub> to a fluorobenzene solution of 3 caused a color change of the solution from black to intense purple, which was attributed to the generation of a Ce<sup>IV</sup>=N moiety. The evaporation of volatiles and subsequent recrystallization of the product from a

mixture of dimethoxyethane and hexanes gave the air- and moisture-sensitive Ce(IV)–imido complex [K(DME)<sub>2</sub>][Ce=N(3,5-(CF<sub>3</sub>)<sub>2</sub>C<sub>6</sub>H<sub>3</sub>)(TriNOx)] (4, Scheme 2) in yields of up to 28%. The <sup>1</sup>H NMR spectrum of 4, measured in THF-*d*<sub>6</sub>, showed a notably C<sub>3</sub>-symmetric Ce(IV)–TriNOx core, indicating a free rotation about the Ce=N bond and/or de-coordination of the potassium cation on the NMR time scale. Two down-shifted diagnostic resonances observed at  $\delta = 6.09$  and 5.79 ppm were consistent with the aryl protons on the imido aryl group. A downfield shift of the *tert*-butyl signal from  $\delta = 0.78$  ppm in 3 to  $\delta = 1.09$  ppm in 4 was also observed. The diastereotopic methylene proton resonances of the TriNOx ligand in 4 ( $\delta = 3.91$  and 2.24 ppm) were shifted compared to the related values detected for 3 ( $\delta = 4.55$  and 2.85 ppm).

To date, attempts to obtain a charge-separated salt of the imido complex by the encapsulation of the alkali metal cation upon addition of 18-crown-6 to a THF solution of 4 have led to formation of complex 3 and other unidentified products. This observation indicates the expected stabilization of the Ce=N bond by the potassium ion. The electronic absorption spectrum for 4 had broad, low-energy transitions that were reproduced with four Gaussian bands (Figures S2 and S3). These were characterized as ligand-to-metal charge-transfer transitions, consistent with an f<sup>0</sup> Ce(IV) cation in 4.<sup>14</sup>

An X-ray diffraction study confirmed binding of the potassium cation with the Ce=N bond (Figure 2a,b). Additionally, the K(1) ion was surrounded by two chelating DME molecules. The

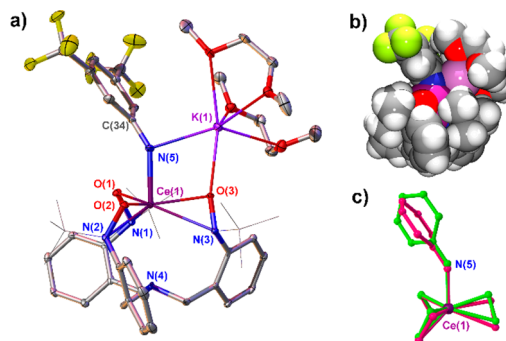


**Figure 2.** (a) Thermal ellipsoid plot of 4 shown at the 30% probability level. Hydrogen atoms and minor disorder components have been omitted for clarity. *tert*-Butyl groups are depicted using a wire model. (b) Space-filling model for 4. (c) Superposition of the Ce(IV) coordination environments of 4 (purple) and 3 (green). Selected bond distances (Å) and angles (deg) for 4: Ce(1)–O(1) 2.231(3), Ce(1)–O(2) 2.234(2), Ce(1)–O(3) 2.277(2), Ce(1)–N(1) 2.620(3), Ce(1)–N(2) 2.621(3), Ce(1)–N(3) 2.640(3), Ce(1)–N(5) 2.119(3), K(1)–N(5) 2.732(3), K(1)–O(3) 2.642(2); Ce(1)–N(5)–C(34) 144.0(3), Ce(1)–N(5)–K(1) 106.30(13), Ce(1)–O(3)–K(1) 104.60(9).

Table 1. Calculated (B3LYP/6-31G\*) and Experimental Geometrical Parameters (Bonds in Å and Angles in deg) for 3, 4, and 4<sup>-</sup>

	3		4		4 <sup>-</sup>
	calcd	exptl <sup>b</sup>	calcd	exptl	calcd
Ce(1)–N(5) <sup>a</sup>	2.328	2.379(3)	2.069	2.119(3)	2.029
Ce(1)–NO <sub>TriNOx</sub>	2.619–2.632	2.510(3)–2.541(3)	2.683–2.740	2.620(3)–2.640(3)	2.761–2.771
Ce(1)–O <sub>TriNOx</sub>	2.196–2.209	2.158(3)–2.203(2)	2.232–2.306	2.231(3)–2.277(2)	2.267–2.270
Ce(1)–N(4)	3.066	2.934(3)	3.336	3.138(3)	3.507
K(1)–N(5)	–	–	2.809	2.732(3)	–
Ce(1)–N(5)–C(34)	140.9	143.3(2)	161.5	144.0(3)	177.5

<sup>a</sup>For assignment of atoms see Figures 1 and 2. <sup>b</sup>For the 3·THF solvate.

important feature of 4 is the presence of an asymmetric four-centered core comprising the Ce(IV) cation, imido-nitrogen, potassium cation, and oxygen O(3) atoms. The Ce–N<sub>imido</sub> bond length of 2.119(3) Å is significantly shorter than that found in 3 (2.379(3) Å) and represents the shortest known Ce–N bond distance, which is indicative of double bond character. This bond length is comparable to the previously reported bridging Yb<sup>III</sup>–N<sub>imido</sub> (2.122(2) Å)<sup>5e</sup> and Sm<sup>III</sup>–N<sub>imido</sub> (2.152(8) and 2.271(7) Å)<sup>5f</sup> distances, after accounting for the difference in ionic radii and assuming a coordination number of 6 for both cations.<sup>15</sup> Elongation of the apical intramolecular Ce(1)–N(4) contact was observed for 4 (3.138(3) Å) compared to 3 (2.934(3) Å). Coordination of the potassium ion to the O(3) atom results in elongation of the Ce(1)–O(3) bond (2.277(3) Å) compared to the two remaining Ce(1)–O<sub>TriNOx</sub> interatomic distances (2.234(3) and 2.231(3) Å). The Ce–N<sub>imido</sub>–C<sub>ipso</sub> bond angle of 144.0(3)<sup>o</sup> is close to that measured in 3 and shows a pronounced deviation from linearity due to the interaction between the potassium cation and the imido core (Figure 2c).

To further understand the nature of the Ce=N bond and the distribution of electron density in 4, we performed calculations on complexes 3 and 4 as well as complex 4 with its potassium cation removed, [Ce=N(3,5-(CF<sub>3</sub>)<sub>2</sub>C<sub>6</sub>H<sub>3</sub>)(TriNOx)]<sup>-</sup> (4<sup>-</sup>), at the B3LYP/6-31g\* level of theory with a 28-electron small-core pseudopotential on Ce. There was general agreement between the key geometrical features of the experimentally determined and calculated structures (Table 1). However, the calculated Ce(1)–N(5)–C<sub>ipso</sub> bond angle of 4 (161.5<sup>o</sup>) was ~17<sup>o</sup> larger than that in the experimentally determined structure. For the anion 4<sup>-</sup>, with an uncompensated negative charge, the corresponding angle was calculated at 177.5<sup>o</sup>. These results indicate that the Ce(1)–N(5)–C<sub>ipso</sub> bond angle showed a rather flat energy surface that was impacted by intermolecular packing forces in the solid state, supporting only weak  $\pi$ -bonding interactions in 4.

Mayer bond order analyses for Ce(1)–N(5) showed an increase from a value of 0.80 for 3, to 1.52 for 4, and 1.70 for 4<sup>-</sup>, which implied a progressively increasing double bond character between the Ce and N atoms. Analysis of the orbital contributions to the Ce(1)=N(5) bonding was consistent with strong polarization of the bond. Natural population analyses showed that there was a natural charge on Ce of 1.86 in 3, 1.78 in 4, and 1.79 in 4<sup>-</sup>. There was also a change in the natural charges on the N<sub>imido/anilide</sub> from -0.92 in 3 to -0.95 and -0.88 in 4 and 4<sup>-</sup>, respectively. Natural Bond Orbital analysis was also performed. As expected, the bonding molecular orbitals involved in the Ce(1)–N(5) bond in 3 were mainly located on the nitrogen atom (89.96%), with the Ce atom contribution (10.04%) split between its 5d (62.41%) and 4f (27.15%) orbitals (Figure 3). Two bonding interactions were observed in 4: a  $\sigma$ -

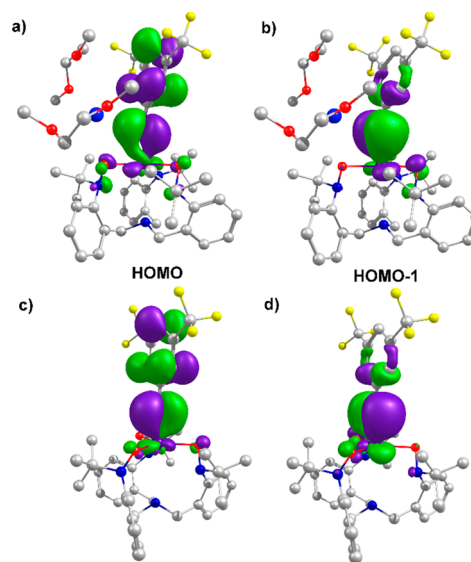


Figure 3. Plots of the Kohn–Sham orbitals, HOMO and HOMO–1 for (a,b) 4 and (c,d) 4<sup>-</sup> based on the optimized structures.

type interaction showed nitrogen and Ce contributions of 87.35% and 12.65%, respectively. A breakdown of the Ce bonding orbital showed that the 5d orbital contributed more than half (56.47%), while the 4f orbital contributed 32.78%. Similarly, the  $\pi$ -type bonding orbital in 4 was mainly of nitrogen character (81.9%), with 18.1% located on Ce. The Ce orbital contributions were also more 5d (53.58%) in character than 4f (46.34%). Complex 4<sup>-</sup> also had two bonding interactions, with a Ce contribution of 13.84% to the  $\sigma$ -type bond. This contribution was mainly of 5d character (54.8%), with some 4f contribution (33.51%). The Ce(IV) ion had a contribution of 19.65% to a  $\pi$ -type interaction, also with more 5d (52.86%) than 4f (47.06%) character.

The nucleophilic character of the Ce=N fragment in complex 4 was demonstrated by its reaction with the electrophilic substrate, Me<sub>3</sub>SiCl (Figure 4). The yield of the Ce-containing product, Ce(TriNOx)[N(SiMe<sub>3</sub>)(3,5-(CF<sub>3</sub>)<sub>2</sub>C<sub>6</sub>H<sub>3</sub>)] (5), was estimated to be 90% by <sup>1</sup>H NMR spectroscopy upon comparison with an internal standard. Complex 5 was also prepared independently by a synthetic route analogous to the preparation of 2 (see Supporting Information for details). Additionally, the reaction between 4 and pyridinium chloride in THF led to the immediate formation of complex 3.

The molecular structure of 5 is shown in Figure 4. The binding of the trimethylsilyl group to the imido nitrogen atom resulted in the elongation of the Ce(1)–N(5) bond by ~0.2 Å in 5 compared to complex 4. The angle Ce(1)–N(5)–C(34) was significantly smaller in 5 than in the imido complex 4



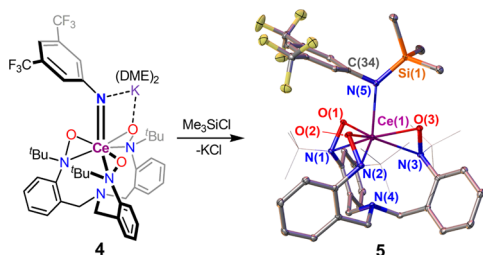


**Figure 4.** Preparation and thermal ellipsoid plot for **5** shown at the 30% probability level. Hydrogen atoms have been omitted for clarity. *tert*-Butyl groups are depicted using a wire model. Selected bond distances (Å) and angles (deg): Ce(1)–O(1) 2.1795(13), Ce(1)–O(2) 2.1766(14), Ce(1)–O(3) 2.1818(14), Ce(1)–N(1) 2.5525(16), Ce(1)–N(2) 2.5602(16), Ce(1)–N(3) 2.5550(16), Ce(1)–N(5) 2.3803(17), Si(1)–N(5) 1.7358(18); Ce(1)–N(5)–C(34) 110.43(12).

(110.43(12)° vs 144.0(3)°, respectively) because of the  $sp^2$  hybridization for the N(5) atom and steric repulsion from the  $-\text{SiMe}_3$  group. Restricted rotation about the N(5)–C(34) bond led to desymmetrization of the 3,5-( $\text{CF}_3$ ) $_2\text{C}_6\text{H}_3$  fragment according to NMR spectroscopy (see [Supporting Information](#)).

In summary, we have isolated a unique tetravalent cerium complex containing a Ce=N bond. The weak coordination of an alkali metal cation to the nucleophilic center in the Ce=N unit provided a stabilizing effect in addition to the steric hindrance of the  $\text{TriNO}_3^-$  ligand framework and electron-withdrawing 3,5-( $\text{CF}_3$ ) $_2\text{C}_6\text{H}_3$  substituent. DFT computations supported the Ce=N character in **4** and a larger contribution from 5d orbital character in the valence electronic structure. These results are important for the further exploration of metal–ligand bonds of f-block elements and investigation of their reactivity. We are currently exploring the effects of different alkali metal ions and substituents on the stabilization of a Ce=N bond and the reactivity of the corresponding complexes.

## ■ ASSOCIATED CONTENT

### 📄 Supporting Information

The Supporting Information is available free of charge on the [ACS Publications website](#) at DOI: [10.1021/jacs.6b03293](https://doi.org/10.1021/jacs.6b03293).

Figures S1–S15 and Tables S1–S5, details of experimental procedures, structural and theoretical investigations, multinuclear NMR and UV–vis spectra, and crystallographic files ([PDF](#))

X-ray crystallographic data for 2–5 ([CIF](#))

## ■ AUTHOR INFORMATION

### Corresponding Author

\*[schelter@sas.upenn.edu](mailto:schelter@sas.upenn.edu)

### Notes

The authors declare no competing financial interest.

## ■ ACKNOWLEDGMENTS

We thank the National Science Foundation (CHE-1362854) and University of Pennsylvania for financial support of this work. L.A.S. thanks the NSF Graduate Research Fellowship program for support. We also thank K. C. Mullane and Dr. H. Yin (University of Pennsylvania) for helpful discussion.

## ■ REFERENCES

- (1) Nugent, W. A.; Mayer, J. M. *Metal-Ligand Multiple Bonds*; Wiley-Interscience: New York, 1988.
- (2) (a) Basuli, F.; Bailey, B. C.; Tomaszewski, J.; Huffman, J. C.; Mindiola, D. J. *J. Am. Chem. Soc.* **2003**, *125*, 6052. (b) Hazari, N.; Mountford, P. *Acc. Chem. Res.* **2005**, *38*, 839. (c) Aktas, H.; Slootweg, J.; Lammertsma, K. *Angew. Chem., Int. Ed.* **2010**, *49*, 2102. (d) Svitova, A. L.; Ghiassi, K. B.; Schlesier, C.; Junghans, K.; Zhang, Y.; Olmstead, M. M.; Balch, A. L.; Dunsch, L.; Popov, A. A. *Nat. Commun.* **2014**, *5*, 4568.
- (3) (a) Upton, T. H.; Rappe, A. K. *J. Am. Chem. Soc.* **1985**, *107*, 1206. (b) Geyer, A. M.; Wiedner, E. S.; Gary, J. B.; Gdula, R. L.; Kuhlmann, N. C.; Johnson, M. J. A.; Dunietz, B. D.; Kampf, J. W. *J. Am. Chem. Soc.* **2008**, *130*, 8984. (c) Odom, A. L. *Dalton Trans.* **2011**, *40*, 2689.
- (4) (a) Evans, W. J.; Kozimor, S. A.; Ziller, J. W. *Science* **2005**, *309*, 1835. (b) Bart, S. C.; Anthon, C.; Heinemann, F. W.; Bill, E.; Edelstein, N. M.; Meyer, K. *J. Am. Chem. Soc.* **2008**, *130*, 12536. (c) Ren, W.-S.; Zi, G.-F.; Fang, D.-C.; Walter, M. D. *J. Am. Chem. Soc.* **2011**, *133*, 13183. (d) King, D. M.; Tuna, F.; McInnes, E. J. L.; McMaster, J.; Lewis, W.; Blake, A. J.; Liddle, S. T. *Science* **2012**, *337*, 717. (e) Lewis, A. J.; Carroll, P. J.; Schelter, E. J. *J. Am. Chem. Soc.* **2013**, *135*, 511. (f) Hayton, T. M. *Chem. Commun.* **2013**, *49*, 2956. (g) Mullane, K. C.; Lewis, A. J.; Yin, H.; Carroll, P. J.; Schelter, E. J. *Inorg. Chem.* **2014**, *53*, 9129. (h) Anderson, N. H.; Odoh, S. O.; Yao, Y.; Williams, U. J.; Schaefer, B. A.; Kiernicki, J. J.; Lewis, A. J.; Goshert, M. D.; Fanwick, P. E.; Schelter, E. J.; Walensky, J. R.; Gagliardi, L.; Bart, S. C. *Nat. Chem.* **2014**, *6*, 919. (i) Anderson, N. H.; Yin, H.; Kiernicki, J. J.; Fanwick, P. E.; Schelter, E. J.; Bart, S. C. *Angew. Chem., Int. Ed.* **2015**, *54*, 9386. (j) Behrle, A. C.; Castro, L.; Maron, L.; Walensky, J. R. *J. Am. Chem. Soc.* **2015**, *137*, 14846. (k) Smiles, D. E.; Wu, G.; Kaltsoyannis, N.; Hayton, T. W. *Chem. Sci.* **2015**, *6*, 3891.
- (5) (a) Masuda, J. D.; Jantunen, K. C.; Ozerov, O. V.; Noonan, K. J. T.; Gates, D. P.; Scott, B. L.; Kiplinger, J. L. *J. Am. Chem. Soc.* **2008**, *130*, 2408. (b) Wicker, B. F.; Scott, J.; Andino, J. G.; Gao, X.; Park, H.; Pink, M.; Mindiola, D. J. *J. Am. Chem. Soc.* **2010**, *132*, 3691. (c) So, Y.-M.; Wang, G.-C.; Li, Y.; Sung, H. H.-Y.; Williams, I. D.; Lin, Z.; Leung, W.-H. *Angew. Chem., Int. Ed.* **2014**, *53*, 1626. (d) Schädle, D.; Meermann-Zimmermann, M.; Schädle, C.; Maichle-Mössmer, C.; Anwänder, R. *Eur. J. Inorg. Chem.* **2015**, *2015*, 1334. (e) Chan, H.-S.; Li, H.-W.; Xie, Z. *Chem. Commun.* **2002**, 652. (f) Gordon, J. C.; Giesbrecht, G. R.; Clark, D. L.; Hay, P. J.; Keogh, D. W.; Poli, R.; Scott, B. L.; Watkin, J. G. *Organometallics* **2002**, *21*, 4726.
- (6) (a) Giesbrecht, G. R.; Gordon, J. C. *Dalton Trans.* **2004**, *16*, 2387. (b) Summerscales, O. T.; Gordon, J. C. *RSC Adv.* **2013**, *3*, 6682.
- (7) (a) Coles, M. P.; Hitchcock, P. B.; Khvostov, A. V.; Lappert, M. F.; Li, Z.; Protchenko, A. V. *Dalton Trans.* **2010**, *39*, 6780. (b) Gordon, J. C.; Giesbrecht, G. R.; Clark, D. L.; Hay, P. J.; Keogh, D. W.; Poli, R.; Scott, B. L.; Watkin, J. G. *Organometallics* **2002**, *21*, 4726.
- (8) Lu, E.; Li, Y.; Chen, Y. *Chem. Commun.* **2010**, *46*, 4469.
- (9) Gregson, M.; Lu, E.; McMaster, J.; Lewis, W.; Blake, A. J.; Liddle, S. T. *Angew. Chem., Int. Ed.* **2013**, *52*, 13016.
- (10) (a) Bogart, J. A.; Lippincott, C. A.; Carroll, P. J.; Schelter, E. J. *Angew. Chem., Int. Ed.* **2015**, *54*, 8222. (b) Bogart, J. A.; Lippincott, C. A.; Carroll, P. J.; Booth, C. H.; Schelter, E. J. *Chem. - Eur. J.* **2015**, *21*, 17850.
- (11) Williams, U. J.; Robinson, J. R.; Lewis, A. J.; Carroll, P. J.; Walsh, P. J.; Schelter, E. J. *Inorg. Chem.* **2014**, *53*, 27.
- (12) Crozier, A. R.; Bienfait, A. M.; Maichle-Mössmer, C.; Törnroos, K. W.; Anwänder, R. *Chem. Commun.* **2013**, *49*, 87.
- (13) Vroegop, C. T.; Teuben, J. H.; van Bolhuis, F.; van der Linden, J. G. M. *J. Chem. Soc., Chem. Commun.* **1983**, 550.
- (14) (a) Bogart, J. A.; Lewis, A. J.; Medling, S. A.; Piro, N. A.; Carroll, P. J.; Booth, C. H.; Schelter, E. J. *Inorg. Chem.* **2013**, *52*, 11600. (b) Dorfner, W. L.; Carroll, P. J.; Schelter, E. J. *Dalton Trans.* **2014**, *43*, 6300. (c) Schneider, D.; Spallek, T.; Maichle-Mössmer, C.; Törnroos, K. W.; Anwänder, R. *Chem. Commun.* **2014**, *50*, 14763.
- (15) Shannon, R. D. *Acta Crystallogr., Sect. A: Cryst. Phys., Diffr., Theor. Gen. Crystallogr.* **1976**, *32*, 751.